On-Site Raman Spectroscopic Study of Beads from the Necropolis of Vohemar, Northern Madagascar (>13th C.)

Philippe Colomban [1,*], Gulsu Simsek Franci [1,2] and Farahnaz Koleini [3,4]

1. MONARIS UMR8233, Sorbonne Université, CNRS, 75005 Paris, France; gusimsek@ku.edu.tr
2. Rumelifeneri Campus, College of Sciences, Surface Science and Technology Center (KUYTAM), Koç University, Rumelifeneri Yolu, Sariyer, Istanbul 34450, Turkey
3. Department of Anthropology and Archaeology, Faculty of Humanities, University of Pretoria, Pretoria 0028, Gauteng, South Africa; Farahnaz.koleini@up.ac.za
4. Department of Art and Architecture, Faculty of Art, Azad University of Shahin Shahr, Isfahan 65, Iran
* Correspondence: philippe.colomban@sorbonne-universite.fr or philippe.colomban@upmc.fr

Abstract: In the late 19th century, ancient tombs were discovered near the village of Vohemar at the northeastern point of Madagascar, and subsequent excavations during the French period (1896–1945) revealed the presence of a major necropolis active from ~13th to 18th centuries. Some artefacts (Chinese ceramic shards and glass trade beads) recovered from these excavations was sent to France and now in part belong to the collection of the Musée d'Histoire Naturelle, Nimes. Carnelian and glass trade beads were analyzed with a mobile Raman spectrometer, which identified different materials (soda-lime glass, quartz/moganite, carnelian/citrine, chalcedony) and coloring agents (Naples yellow, cassiterite, amber chromophore, transition metal ions, etc.). The results are compared with those obtained on beads excavated at different sites of Southern Africa and at Mayotte Island, and it appears that (most of) the beads come from southern Asia and Europe. The results confirmed the role that northern Madagascar played within the maritime networks of the Western Indian Ocean during the 15th–16th century.

Keywords: beads; carnelian; glass; quartz; pigments; Raman spectroscopy; trade

1. Introduction

1.1. Historical, Ethnical and Geographical Context

With the syntheses of Baujard [1] it is now well established that even before medieval times the Indian Ocean was, thanks to the maritime traffic allowed by the monsoon winds, a place of exchange between different continents, Asia with India and Malaysia in direct contact with China, the Arabian Peninsula and the Iranian coast (Hormuz) in connection with the Mediterranean world and many trading posts along the African coast [2–6]. The necessary use of the monsoon winds made northern Madagascar and the entrance to the Mozambique Channel the most distant points navigators could reach without having to wait for another cycle to set off again. Vohemar, a natural harbor located on the eastern coast of the northern tip of Madagascar Island, was therefore one of the possible relay points for trade along the coast to southern Africa [5–7].

Vohemar is known in the Arab-Malagasy texts by the name of *Bimaro* or *Iharana*; the inhabitants of this site being called *Rasikajy* by the Malagasy. In the late 19th century, ancient tombs were discovered near the village of Vohemar [8]. Subsequent excavations and research revealed the presence of a major necropolis attributed to a prosperous *Rasikajy* group [9]. The particular link of the *Rasikajy* civilization with Asia (Chinese or Austronesian groups in Srivijaya) has been proposed on the basis of skeletons and particular utensils found in the cemetery [10]. The necropolis dates back to at least the 13th century and was still in use when the first Europeans visited the region in the early 16th century.

The catalogue of Vernier and Millot [9] presented the objects coming from the excavations carried out between 1885 and 1941, mainly by Godebout and Vernier in the ancient cemetery, whose tombs oriented east–west with the faces of the skeletons oriented towards Mecca: these comprise tripod pots in "Chinese" shapes in so-called chloritoschist, steatite or soapstone, objects in metal (silver alloy and gold rings, bronze mirrors and utensils), bone/ivory and mother-of-pearl, Chinese ceramics (celadons, stoneware, monochrome, blue-and-white and *sancai* porcelain), copal resin as well as glass fragments and a large number of bead necklaces and bracelets. Additional information can be found in the Vérin thesis and book [11]. A ^{14}C dating gave a period around the 13th century. The ceramics are well preserved and were recently the subject of a re-investigation by Zhao in 2011 [12], which confirmed the attributions of Vernier and Millot to the end of the Yuan and Ming Dynasties ceramics, some artefacts having Emperor reign marks, mostly dating from the 14th to the end of the 16th century. Five Spanish lustre pots (likely originating from the Paterna or Manises kilns, close to Valencia) dating from the end of the 15th century or beginning of 16th century were also identified by Amigues [13].

Vérin [11] proposed first that the *Rasikajy* civilization was the result of biological and cultural intermingling between Islamized groups (Swahili) arriving at the island and establishing many outposts along the African coast [1] and local (female) people already present in northeast Madagascar. The position of the dead in the tombs at the graveyard of Vohemar has been used to confirm that the civilization had Muslim roots, and the presence of imported pottery indicates strong engagement in the maritime trade with the East across the Indian Ocean [14]. Vernier and Millot [9] considered that most imported pottery found in the tombs dates from between the 14th and 16th centuries CE. In contrast, Vérin [11], who only had a limited access to objects excavated at Vohemar, concluded that the finds date mostly from c. 1400 up to 1750 CE.

In 2011 Allibert and Rakotoarisoa, in their preface to a special issue of *Etudes océan Indien* dedicated to Vohemar [15], explained the naming Vohemar: the name of Sultan *Bimar* (meaning "sick") was transformed into *Bimaro* then *Vohemar* by the first Europeans (the real name being *Iharana*). Etymologically, *Rasikajy* could have come from *Ra-Si-Hadjy* "*the cape of Muslim pilgrims*"; another potential explanation comes from the Swahili language in which *Rasi* mean cape and *Kadjy* means sand hill, which is consistent with the local geography.

1.2. Trade Beads Excavated at Vohemar

In this paper, we examine the beads of the Nimes collection on-site with a mobile Raman microspectrometer. The Nimes Museum collection consists of the artefacts (the choice undoubtedly fell on the objects considered as the prettiest) collected by Maurein from 1904 to 1913 and given as a bequest. The beads are presented packaged in necklaces and bracelets, in principle to mimic their initial arrangement on the skeletons, but certainly to make the exhibition more interesting for visitors. The collection was examined in 1960 by Van der Sleen [16], a renowned expert in trade beads [5,17]. A considerable number of the objects coming from the ~1000 excavated tombs were also sent afterwards to the Musée de l'Homme, Paris (and are now at the Musée du Quai Branly-Jacques Chirac) and some of them can be viewed online (http://www.quaibranly.fr). The paper of Rasoarifetra [18] reported on the 22,474 beads excavated by Gaudebout and Vernier in 1941 and preserved at the Institut de civilisations/Musée d'art et d'archéologie de l'Université d'Antananarivo, Madagascar. They were also part of the necklaces and bracelets found on the skeletons before. By visual inspection Rasoarifetra identified 139 beads as made of coral, 155 of carnelian, 65 of rock crystal (quartz) and 21,775 of glass, plus a few beads made of copper, gold and silver.

Three types of "glass" beads, respectively made of opaque "glass," translucent "glass" and transparent glass, have been distinguished in previous studies. Opaque red to brown beads (Figure 1d) are called *mutisalah* or "Indian red" and constitute about 50% of the entire collection in Antanarivo and, according to reference [18], they were sold in Sumatra as early as the 1st century CE. They have also been identified as "monsoon beads" [19,20].

Rasoarifetra [18] recognized two types of glass composition in the Malagasy bead collections, and these are believed to have been used in both South and Southeast Asia. The mineral-soda glass, the first type of glass, would have circulated between the 11th and 13th centuries in the Indian Ocean and later on, between the 15th and the 17th centuries, in the Shashi-Limpopo region. The mineral-soda glass was marketed until the 17th century on the eastern coast of Africa [19,20]. The second type, plant-ash glass, was known in the Shashe-Limpopo and Zimbabwe regions during the period from the second half of the 13th to the first half of the 15th century, but was already marketed in southern Africa between the 8th and mid–10th centuries [5].

Robertshaw et al. [19] analyzed the elemental composition of two series of beads from the same period excavated in two sites located on the western and eastern coast of the North of Madagascar, at Mahilaka and Sandrakatsy, respectively. The second place is not far away from Vohemar, but inland and considered to have been also founded by the first immigrants from Southeast Asia. Plant-ash (characterized by both high MgO > 2.5 %wt and high CaO content) and mineral-soda (characterized by a low MgO (< 1.5 %wt) and high Al_2O_3 level, ~12 %wt) are in evidence, both with a variety of colors and assigned to an origin from southern Asia. Similar soda-lime-silica glass beads have been found in Kenya [21]. They belong to the high alumina-plant ash glass type, characterised by high alumina and relatively low calcium contents, widely distributed in eastern (10th–16th centuries CE) and southern Africa (13th–15th centuries AD), Central Asia (9th–14th centuries CE) and Southeast Asia (12th–13th centuries AD), made with plant ash and sand. Plant-ash glass beads are blue, green, yellow, and clear. Mineral-soda glass beads are yellow, black, brownish-red, blue-green, yellowish-green, reddish-brown, and clear. The Malagasy plant-ash glass beads are rather similar to those of Kota Cina, an important 12th–14th century harbor site in northern Sumatra [22]. A blue bead with lower MgO and Al_2O_3 levels looks like part of the Zhizo series [20,23–25]. Four blue plant-ash glass beads show rather large amounts of As_2O_3 (the CoO/As_2O_3 ratio ranges between 0.9 and 1.4), slightly elevated MnO content and are almost Ni- and Zn-free. This is consistent with the use of cobalt ore (cobaltite) from Rajasthan, i.e., for an Indian and/or Central Asian production.

The collection of beads at Nimes includes carnelian and glass beads plus particular multicolored "*herringbone*" beads (also called "*chevron*" beads [26]) not observed in the sites of southern Africa or the islands of the Comores [5–7]. We will identify the materials (mineral or glass) and the coloring agents/pigments and compare with the beads excavated in southern Africa and Mayotte, which have been previously analyzed by Raman microspectrometry. This preliminary work was undertaken in order to evaluate the collection and to stimulate interest in the performing of more sophisticated analyses.

2. Materials and Methods

2.1. Beads

The collection at Nimes Natural History Museum consists of about 1100 beads displayed in the form of seven necklaces and four bracelets. The analyzed artefacts are listed in Table 1 and are shown in Figure 1. Previous studies categorized the beads as being made of carnelian, glass and "terracotta," most of them (~75%) being in gemstones belonging to the carnelian (and/or the citrine, as we will see further) series, being composed of a microcrystalline to monocrystalline, optically translucent to clear silica colored by Fe^{2+} ions. The proportion of materials is therefore very different from what was indicated by Rasoarifetra for beads preserved in Antanarivo [18]. It is probable that a selection of the "most beautiful" necklaces/bracelets was previously made by Maurein for his collection, which was brought back to France.

About a hundred beads were analyzed here by Raman microscopy. Figure 1 shows the variety of beads studied: 10 types can be recognized from a visual examination:

(i)   orange to red, optically clear gemstones with tubular, more or less spherical or oval, bi-conical shapes (Figure 1a'–c,f),

(ii)   optically clear to milky colorless spherical beads (Figure 1a',c,f),

(iii)   translucent (Figure 1a',c,f) to optically clear (Figure 1a') green beads,

(iv)   opaque (Figure 1c,f) green beads,

(v)   opaque (Figure 1c) turquoise beads,

(vi)   yellow opaque beads (Figure 1a',c,f),

(vii)   multicolor (blue-white-red) *"herringbone"*/*chevron* beads (Figure 1a',b,f),

(viii)   opaque gray to black beads (Figure 1d–g), some of them previously categorized as terracotta,

(ix)   opaque blue on white body prisms, rather similar to those called Nueva Cadiz beads, often associated to chevron beads [27,28] (Figure 1a',c,f,h).

(x)   red opaque beads (Figure 1g), previously categorized as terracotta in the catalogue.

Many of the abovementioned beads (black, brownish-red, grey, yellow) look like members of the East Coast and Khami Indo-Pacific series excavated at archaeological sites in southern Africa such as K2, Mabungubwe and Khami period sites [5,19,20,22–25]. It seems some of these "grey" beads could have been corroded or burned.

Carnelian and rock crystal beads are shaped, spherical or faceted: termed bi-conical, bi-tronconical, pear-shaped, lozenge, faceted tabular according the classification by Beck [29] and taken up by Dubin [30]. Carnelian and agate beads were produced in India and Pakistan and traded very early across the Indian Ocean [31–37]. According to Rasoarifetra, worked patterns [18] including the faceted type are characteristic of the production at the Indian city of Cambay [9,31–37], the facets giving the stone a particular sparkle. In general, carnelians have six facets while clear quartz has eight. The color of carnelian varies from light translucent or opaque orange to dark orange. Similar beads have been found in many harbors around the Indian Ocean, especially at the entrance of the Mozambique Channel [5,37,38]. The presence of half-worked nodules and beads comprising a single threading hole in the graves of Vohemar as in Kilwa led Bernard-Thierry [39,40] to issue a hypothesis on the existence of a local stone processing workshop, at least for the perforation or recovery of raw material. Indeed, the occurrence of quartz crystals (and gold, silver, copper, and iron) is widespread throughout northeastern Madagascar, many of them being found close to the harbor of Vohemar. Large single crystals of quartz were industrially mined after 1945 for applications in electronics and electrotechnics. Therefore, according to Schreuers and Rakotoarisoa [41], it is likely that gold, silver, copper, iron and quartz objects found in the tombs at Vohemar were not only worked locally by the *Rasikajy*, but also produced from raw materials mined in the Vohemar region and exported. The exportation of Malagasy rock crystal by Swahili merchants has been well documented [42].
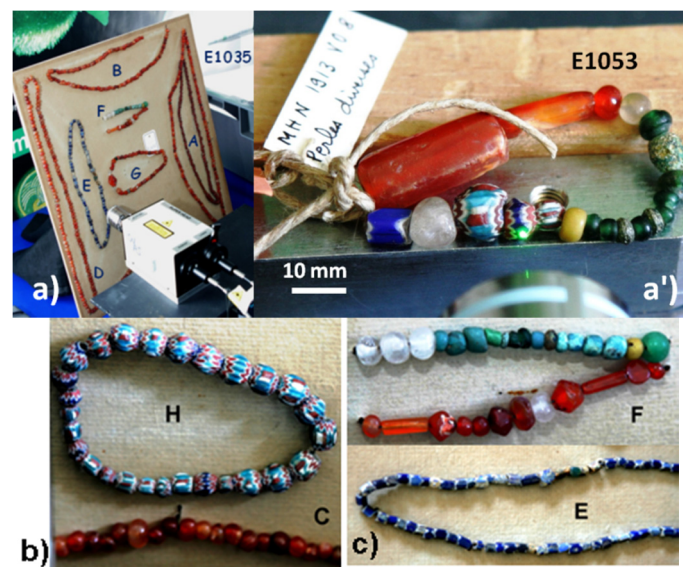

Figure 1. *Cont.*

Figure 1. Beads excavated at Vohemar cemetery (Nimes Museum Collection): (**a**) non-destructive analysis using a remote Raman 532nm Superhead® probe (see the green laser spot in (**a′**) on a multicolored bead from E1053); (**b–h**) details of objects (C,E,F and H bracelets (**b**,**c**) belong to E1035 group). The sample designation is given in Table 1. See details in Figure 2.

Table 1. Description of gemstone and glass beads from Vohemar (Nimes Museum records).

Designation	Description	Bead Number	Figure	Materials	Remarks
E1035: A, B, C, D, E, F, G	Necklaces and bracelets	A_{centre} = 131 (7 tubes) A_{ext} = 114 B = 107 C = 113 D = 145 E = 82 (blue chevron prisms) F = 30 (4 colorless, 9 turquoise, 4 green, 1 yellow) G = 63 (4 colorless, 1 black, 1 multi, 1 white and red) H = 27 multicolor *"herringbones"* and Nueva Cadiz beads	1a,b,c	Carnelian and glass	mean diameter: 3 to 5 mm
E1053 (MHN 1913 V08)	Bracelet	20 (2 tubes, 1 prism, 2 colorless, 3 multi, 1 yellow, 7 green, 3 grey)	1a′,f	Glass	mean diameter: 3 to 10 mm
E1057	Necklace	~250	not shown	Carnelian	not shown, similar to E1035D
E1058	Isolated beads	9 black	d		mean diameter 4 to 6 mm

Table 1. *Cont.*

Designation	Description	Bead Number	Figure	Materials	Remarks
E1059	2 Bracelets	17 (red and black) 15 black	g	Terra cotta	
E1060	Isolated beads	2 grey	e		mean diameter 10 mm
"Indiennes"	Bracelet	17 + 1 (blue chevron prisms)	a',c,h		

2.2. On-Site Raman Microspectroscopy

The transportation of these artefacts to the laboratory not being possible, artefacts were analyzed using a portable HE532 (Horiba Scientific-Jobin Yvon, Longjumeau, France) spectrometer equipped with a Peltier effect-cooled CCD detector and connected by optic fibers with two 532 nm Nd/YAG Ventus laser (Quantum, UK), one with a maximum output power of 80 mW (for dark-colored beads) or a second laser with a 300 mW maximum output (for optically clear and light colored beads) for analysis (Figure 1). The power at the sample was less than 10% of the output laser power and adjusted by controlling the laser power and a diaphragm at the entrance of the remote head ranging between 1 (black sample) and 20 mW (colorless material).

The mobile HE532 instrument offered a combination of a very high sensitivity and rather good resolution (920 lines/mm grating that led to ~4 cm^{-1}). Indeed, recording the spectrum of a vitreous silicate, in particular, on objects from archaeological excavations, is difficult because the surface of the object has lost its optical qualities and the spectrum of a vitreous silicate consists of broad bands. The focal length was 300 mm and fixed spectral window was 60–3200 cm^{-1}. The remote SuperHead® (Horiba Jobin-Yvon) was connected by means of optic fibers to the HE532 spectrometer and equipped with Nikon 50× or Mitutoyo 50× and 200× long working distance objectives. The analyzed volumes comprised ~3 × 3 × 10 and 0.5 × 0.5 × 3 μm^3, respectively; the 17 to 22 mm distance between the front lens and the focal point at the object surface guaranteed the safe condition of recording without any contact being made between the front surface of the objective and the artefact. Analyzed beads are shown at higher magnification in Figure 2.
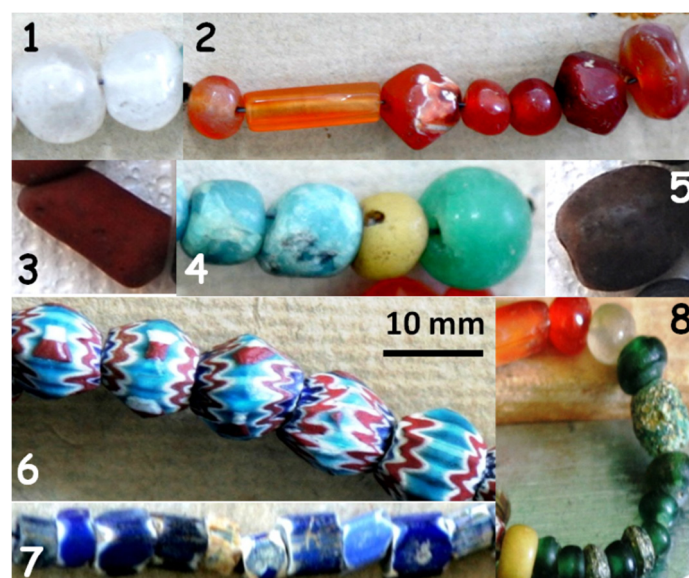

Figure 2. *Cont.*

Figure 2. Detail of the different beads excavated at Vohemar cemetery (Nimes Museum Collection): a star indicates the spot where the analysis was made; nomenclatures used in the text are given; 1, 2 and 4: beads from E1035-F group; 3 and 5, E1059; 6, E1035-H; 7, E1035-E; 8, E1053.

Different spots were tested in order to obtain the spectrum with the best signal/noise ratio and not perturbed by surface ion leaching. The strongest Raman spectra were normally obtained when the focus was close to the optical surface of the sample, but the surface of glass can be subjected to ion leaching and corrosion [43]. However, corrosion strongly decreases the Raman signal and broadens the bands. Typically, between 3 and 5 "good" spectra were recorded for each type of colored area (recording time: 1 to 30s, 100 to 10 spectral accumulations).

3. Results

Figure 3 shows representative as-recorded Raman spectra. Because of the use of optic fibers to connect the remote optical head (Figure 1a) and of edge filters to remove the Rayleigh scattering, a significant background is observed. The background increases regularly up to 400–500 cm^{-1} and then is rather flat. When the Raman spectrum is strong the background contribution is minimal.
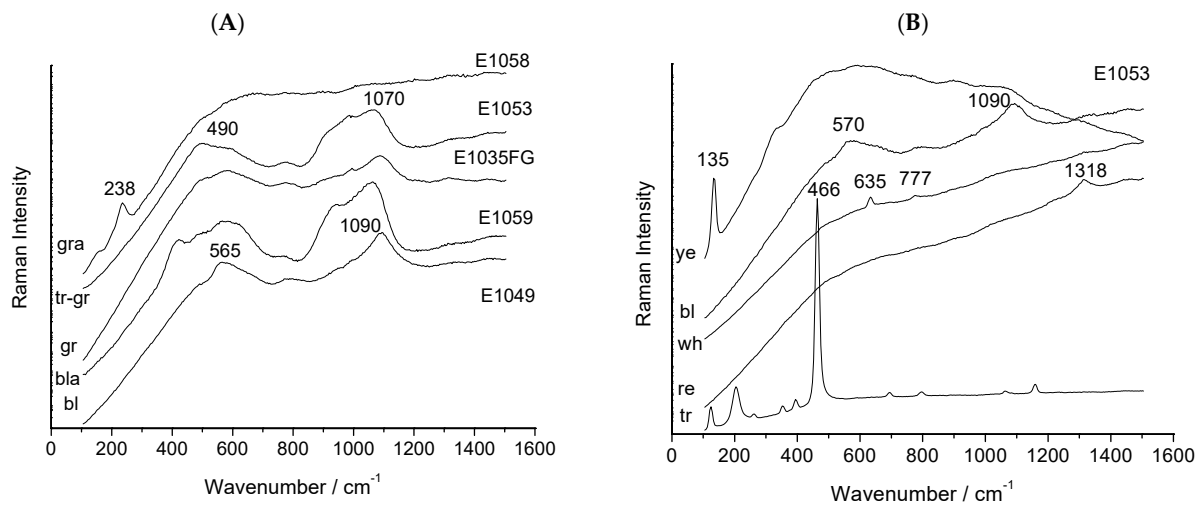
Figure 3. Examples of as-recorded spectra. (**A**): representative spectra exhibiting broad bands; (**B**): variety of spectra recorded on the different colored beads of bracelet E1053 (gra: black/gray to brownish; tr-gr: turquoise-green; gre: green; bla: black; bl: blue; ye: yellow; wh: white; re: red; tr: optically clear and colorless). The background due to the filter transmission and material fluorescence must be subtracted for a better examination of the Raman signature, see Figures 4–7.

The very low background recorded for some beads was consistent with the single crystal character of the bead, e.g., for a quartz bead in the bottom spectrum of Figure 3 and for spectra of Figure 4. As commonly observed, glassy phases exhibited a spectrum made up of broad bands. The Raman intensity strongly depended on several parameters, namely, the amount of the phase giving the spectrum and the nature of the chemical bond: the more covalent the bond, the more electrons involved in the bond, and the larger will be the Raman intensity. The subtraction of the baseline following the established procedure allowed the comparison of spectra recorded with different instruments [44]. Once a convenient quality, a processed spectrum was obtained, if possible, following previously established categorization criteria [44–53], to assign the spectra to a particular mineral or a family of glass bead. Broad components at ~500 and 1000 cm^{-1} were characteristic of the bending and stretching bands of the SiO$_4$ vibrational unit forming the silicate amorphous framework (Figure 3). The wavenumber of the bands and of their components shifted as a function of the fluxes/stabilizers used [45–49]. Additional narrow peaks were characteristic of the crystalline pigments coloring the glass and of the opacifiers used.
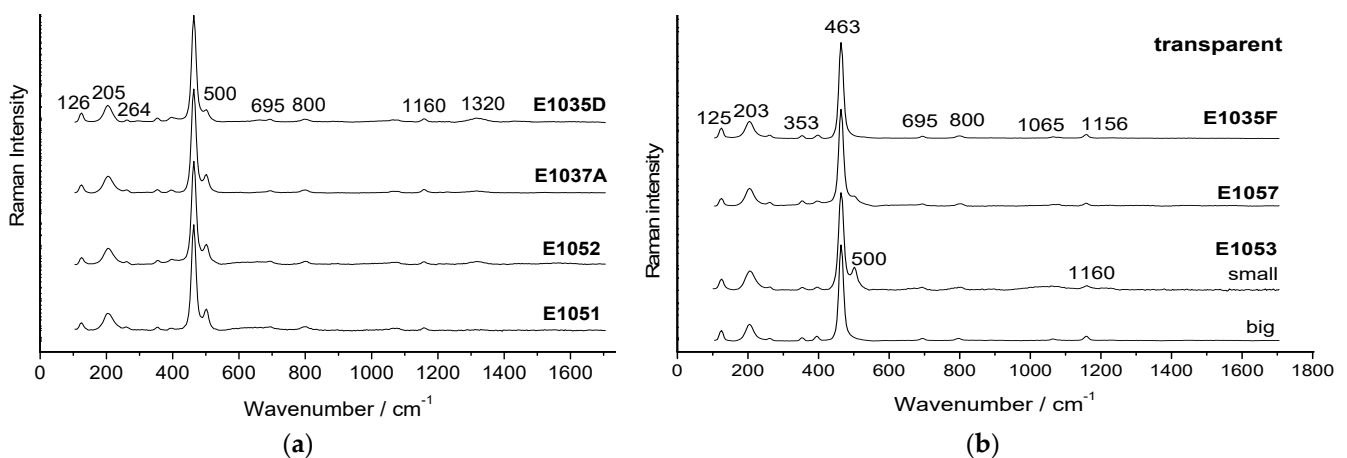
Figure 4. Representative Raman spectra of the different gemstones presented in Figure 1 ((**a**): more or less dark honey color; (**b**): transparent material).

3.1. Gemstone Identification

Due to the very large number of orange to red gemstones, a limited number of beads were selected to be analyzed among those having different degrees of translucency/transparency. Representative spectra are presented in Figures 3 and 4: some beads presented the spectral characteristic of α-quartz (strong 464 cm^{-1} band of the SiO$_4$ bending mode, medium and broad band of the librational 200 cm^{-1} mode, narrow ~1155 cm^{-1} peak, etc. [44–47]), while some others showed an additional more or less intense 500 cm^{-1} peak, which was assigned to moganite (Figure 4), a signature currently observed in chalcedony [54–56] and flint [57], assigned to the contribution of hydroxylated SiO$_4$ tetrahedra distributed in the quartz structure. Chalcedony and flint are silica made of nanocrystals (the additional presence of amorphous material is debated). Recent interest in these phases has arisen from a tentative suggestion to establish proof of the heating of prehistoric tools made of flint (and chert) to optimize their production [57]. Heating at temperatures between 200 and 900 °C led to water elimination, but the amount and kinetics of the "water" loss depends greatly on the sample state (size) [58], and this is commonly used to adjust the color of silicates such as chalcedony [59]. The presence of the moganite peak seemed to correlate with a lower transparency, with a honeyed character of the bead (see the comparison between the spectra of parts a and b in Figure 4).

Carnelian gems have been used since antiquity [56,60–63] and sources are rather well documented for the Mediterranean world [60] and for India [1,2,32–36]. The moganite peak has not been reported previously. Traces of hematite (α-Fe$_2$O$_3$) were evidenced with its characteristic ca. 1320 cm^{-1} peak [64] (see E1035D spectrum, Figure 4). The characteristic of the moganite and hematite peaks could be a criterion to distinguish the beads assigned to carnelian and to discuss in relation with their geological origin in future work. Spectra exhibiting only the quartz signature (464 cm^{-1}) were characteristic of citrine and not of carnelian, although they looked very similar visually and are called carnelian using the visual criterium. Previous assignments should be thus updated. The signature of α-quartz was also observed for colorless (i.e., rock crystal) beads of the bracelets presented in Figure 1a' (E1053big) and (E1035F) and in Figure 2 (#1). A clear quartz spectrum was recorded on the big tubular specimen E1053, dark red (Figure 1f). The potential of the transformation of moganite into quartz to adjust the color during thermal treatment should be considered.

3.2. Glass Matrices

Representative as-recorded spectra are given in Figure 3. Figures 5 and 6 show representative baseline-subtracted spectra. The spectra look rather similar and the signature consists of two bands, the ca. 550 cm^{-1} band assigned to SiO$_4$ bending components of the different SiO$_4$ entities of the more or less polymerized (Si-O)$_n$ framework, and the ca. 1050 to 1090 cm^{-1} SiO$_4$ stretching components [44–47]. The location of the maximum of the SiO$_4$ bending and stretching peak wavenumbers (Table 2) in the general database, which was established from the Raman study of hundreds of different types of glassy silicate (Figure 7), some of them with elemental compositions determined by classical methods, allowed the identification of the different types of glass.

The Raman classification might not have matched exactly with the compositional classification (the thermal history also modifies the glass nanostructure), but at least the following types were identified.

i. The most frequent glass signature was characterized by an SiO$_4$ stretching band peaking at 1085–1090 cm^{-1}, with two well-defined components at 945 and 995 cm^{-1} and bending mode peaking at ~570 cm^{-1} (Figures 3 and 5); this material corresponded to common lime-based glass (typically having a composition with ~10 to 15% Na$_2$O, 8 to 15 CaO, Figure 7). In some cases only one shoulder was observed at 950 or 995 cm^{-1}. Similar signatures were observed among Khami, Mapugunbwe and European beads, according to the Raman classifications of Koleini et al. [5], which were consistent with the Wood denominations [23–25,37,38]. We will see that the addition of European pigments and the style was consistent with Venetian productions.

ii.   Rarer beads showed a spectrum with a stretching band peaking between 1050 and 1060 cm^{-1} with strong shoulders at positions between 930 and 1000 cm^{-1} (green and yellow beads, and black beads). The bending band peak summit downshifted to ~490 cm^{-1}. Such Raman signatures were consistent with a highly depolymerized silicate network, i.e., processing at a lower temperature, a lead-based composition or lime-rich composition (as encountered for one of the so-called Khami Indo-Pacific beads [5]). Rather similar Raman spectra were also observed for European beads made of lead-containing glass.

Table 2. Glass types.

Glass Type	SiO$_4$ Stretching Band/cm^{-1}	SiO$_4$ Bending Band/ cm^{-1}	Remarks
Soda-lime glass (V1)	1085–1090 S ~950 sh; ~995 sh	~560 S	Mediterranean/European (Chevron and Nueva Cadiz beads)
Soda(-lime) glass (V2)	1055–1080 S	490–575 S	European, or Indo-Pacific (Khami)?
Soda(lead)-lime glass (V3)	930–1055 S	495 S	Indo-Pacific/European?

(**a**)   (**b**)
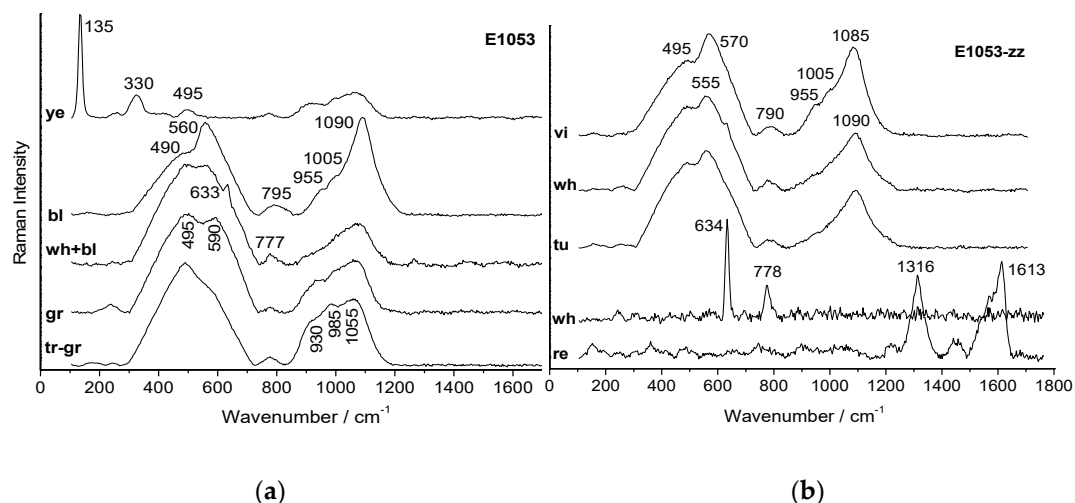
Figure 5. Representative (background subtracted) Raman spectra of the different glass beads presented in Figure 1a',f: left, small beads; right: big *"herringbone"/chevron*(zz) multicolor beads; ye: yellow (similar spectrum obtained for E1035 yellow, Figure 1a'); bl: blue of prismatic Nueva Cadiz beads; wh+bl: white area of blue prismatic beads, see the small SnO$_2$ doublet (Figure 2, bottom); gr: opaque green; tr-gr, transparent green (Figure 2, bottom); vi, violet; tu, turquoise (Figure 1c). For white and red E1053-zz "herringbone" bead bottom spectra, the background subtraction eliminates the contribution of the glass matrix due to the poor quality of the spectra and only SnO$_2$ doublet (wh) and Fe$_2$O$_3$ and carbon (re) signal are detected.

For instance, the spectra of the E1053 necklace reported in Figure 5, right, showed opaque-yellow, blue-white Nueva Cadiz prismatic, blue, violet, white and red *"herringbone"/chevron* beads and turquoise-green beads, which were European. The spectrum of the black beads of the E1059 necklace (Figures 2 and 6) looked similar to those recorded on the Indo-Pacific series, in particular, with a peak around 420 cm^{-1} (see further).
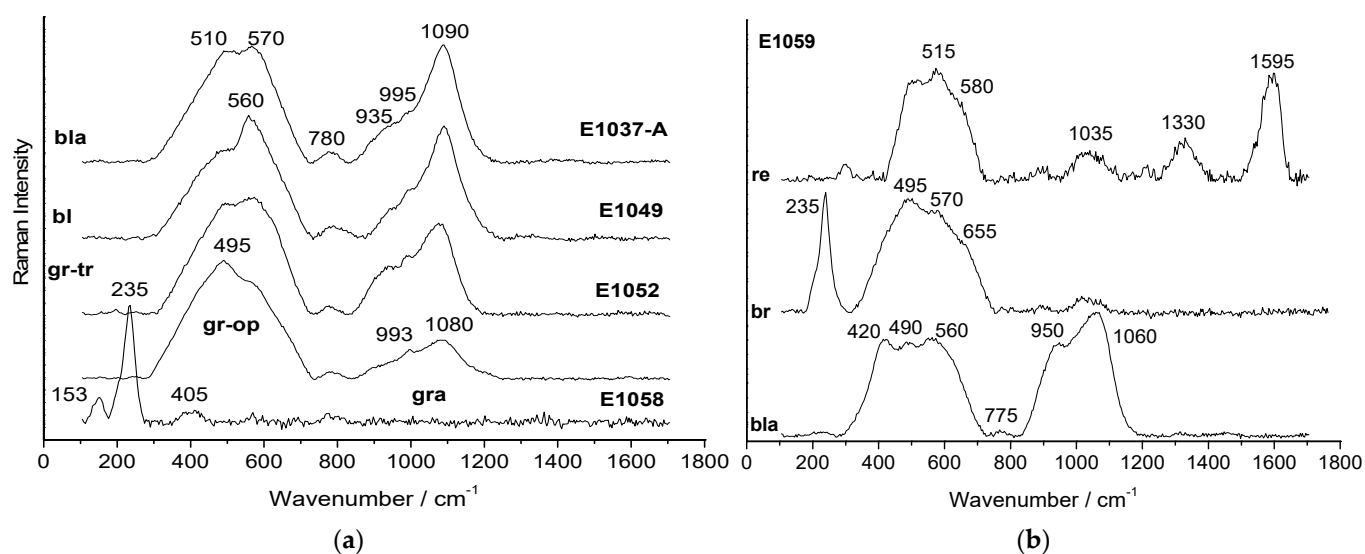
Figure 6. Representative (background subtracted) Raman spectra of the different glass beads presented in Figure 1d,e. See previous figures for labels; bla: black, gr-op: opaque green, gra: grey, br: brown. For the E1059 heavy colored beads, the poor quality of the spectra means that after background subtraction, the contribution of the glassy matrix is strongly distorted or even lost.

3.3. Pigments

Spectra of 60 different beads visually representative of the different colors and shapes were analysed. Figures 5 and 6 show representative Raman spectra of the colored glass beads. Assignments are given in Table 3. The entire Raman signatures were consistent with medieval and post-medieval glass technologies.

The white color was obtained by opacification with cassiterite (SnO_2) [48], characterized by narrow peaks at 635 and 775 cm^{-1}, as observed in the blue and white areas of the multicolored E1053zz "*herringbone*"/chevron and prismatic/Nueva Cadiz blue-on-white beads (Figure 5). The yellow color was achieved using a Naples yellow pigment (narrow peak at ~135 cm^{-1} and 330–495 doublet characteristic of a Sn-rich solid solution ($Pb_{2-x}M'_xM_{2-y}M''_yO_{7-\delta}$, M,M'' = Sb, Sn, Fe, Si, Zn; M' = RE) forming the so-called "defect" pyrochlore [65–76]). These two pigments are a characteristic of European technology developed after the Renaissance/Quattrocento. The red color was obtained with hematite, which was easily identified by the peak at ~1320 cm^{-1} [64]; note the red shade seemed to be controlled by the firing atmosphere, as seen by the observation of carbon doublet at 1350 and 1600 cm^{-1}.

No peaks characteristic of lapis lazuli, cobalt silicate or aluminate as well as arsenates were observed, and the blue color was obtained by dissolution of cobalt in the silicate glassy matrix using European cobalt ores prior to the 17th century or alternatively Asian ores. According to Handcock et al. [77] and Koleini et al. [5,78] the absence of a peak characteristic of the As-O bond (at ~820–830 cm^{-1}) in blue glass is consistent with European production before the middle of the 17th century.

The absence of a specific signature for the green beads was consistent with their coloration by the dissolution of copper ions. The different green shades arose from the matrix effect, i.e., the glass composition (Figure 6), a jade color being obtained for lead-based glass.

Table 3. Coloring agents Raman signatures.

Coloring Agent	Color	Main Peak(s) cm^{-1}	Objects	Figs	Remarks
Hematite (+ carbon)	red	~1320 S (1350–1600 doublet)	E1035 E1059	2, 5, 6, 7	
Naples yellow	yellow	~136 S	E1035 E1053	2, 5, 6	Mediterranean
Cassiterite	white	635 S, 775 m	E1035 E1053	2, 5, 6	Mediterranean
Amber Chromophore (Fe-S-X)	Amber to black	420 S	E1059	7	Mediterranean/Islamic (as Mapungubwe Oblates)
Cu_2O?	gray	235 S	E1058 E1059	7	Asian
Co^{2+}	blue	570 m	E1035	5	

Contrary to the assignment noted in earlier reports, the brown beads of the E1059 bracelet were not made of terracotta but were made of glass colored by hematite (red beads, 1320 cm^{-1} peak) and/or by the amber chromophore (black beads, 420 cm^{-1} peak). The amber chromophore was obtained by the formation of an Fe-S complex. Similar Raman signatures have been obtained on black beads, the oblates of Mapungubwe [53]. The later Mapungubwe beads did not contain metallic copper. It is possible that the beads that appeared red were actually originally black with use of the Fe-S chromophore, and later due to the oxidation (from their being placed in a fire or burning) their color was changed to red. Elemental analysis and/or Raman analysis on a section or fracture are required to characterize these beads more precisely. Spectra of some brown to black beads (Figure 6, E1058, gra; E1059 br) showed a well-defined peak at ~235 cm^{-1}. The exact wavenumber may have been shifted by a few cm^{-1} by the background subtraction procedure, but the peak position fit well with an assignment to cuprite Cu_2O [79]. Cu_2O colors in red, dark red or black as a function of the content were observed, and this pigment was used in some enamels and glazes. Francis [2] first noted the large importation of these beads from Asia. The dark color might have arisen from the oxidative corrosion of the metalic copper dispersed in the glass.

4. Discussion

A large number of beads were made from natural minerals, such as quartz (colorless rock crystal and citrine with a color similar to that of carnelian) and a mixture of quartz and mordenite, characteristic of chalcedony and agate. The qualification of carnelian based on visual criteria mixed these two types of minerals.

Two main origins were identified for glass beads, namely, Asia and Europe. Pigment identification in the multicolor "*herringbone*"/chevron beads confirmed that they were without discussion European. Identification of the Naples yellow pigment gave a date probably after the 15th century. The absence of the signature of an As-O bond on the blue area gave a date before the middle of the 17th century. These dates were consistent with the date assigned to most of the Chinese porcelain (14th–16th centuries) and the Spanish pottery (15th–16th centuries) and with the presence of *chevron* beads (produced after the end of 15th century [26]) and of Nueva Cadiz beads produced after the 16th century [27,28]. They could be associated with Portuguese merchants.

Black beads with signatures rather similar to the Mapungubwe beads supposedly came from the Mediterranean/Islamic and/or Central/South Asia glassmakers. The monochrome glass beads, except for the transparent green ones, were close to the East Coast Indo-Pacific series beads in morphology. These beads were in use in southern Africa from the 11th century AD, except the brownish red and black beads that arrived later into

the region in the middle of the 11th and late 12th century AD, respectively [20,23]. These beads were imported into the region until the middle of the 13th century. Later in the 15th century, a series of beads with a composition close to the East Coast series known as the Khami-IP series was imported to southern Africa. None of the IP black and brownish red beads of southern Africa showed the peak at 235 cm^{-1}, although the beads contained a mixture of copper and iron oxide that might have given the signature of cuprite. The brownish-red beads were thus not similar to those found in southern Africa in terms of the pigment mixture. On-site Raman analysis of opaque materials being limited to the surface, corrosion and/or thermal treatments could explain the different Raman signatures. The Raman spectrum was also different from that recorded on the glass beads colored by copper (most likely copper metal and copper oxide) excavated from Mayotte Island [7]. These beads were corroded on the surface, and it was possible that the different Raman signatures arose from different degrees of degradation. Obviously, the identification of phases by Raman scattering required an analysis of the bulk (section) and not only of the bead surface. Although the Raman signature of some of the beads excavated from Mayotte [7] and South Africa [5] exhibited peaks characteristic of crystalline impurities of raw materials (such as zircon, Cr-Sn silicate with sphene structure), none of the beads in the present study showed similar peaks. The opaque green beads with Raman spectral characteristics of mineral-soda glass (Figure 7) had more similarity with the southern Africa IP series and therefore might be of the same origin. The glass bead of V1 type was located in the area of a typical European glass bead, according to the conclusion based on the identification of coloring pigments. Beads made of V2 type glass also corresponded to the soda-lime group, but the much larger dispersion of the data was consistent with the glasses of different origins, in particular, those of the Khami, Mapungubwe and European series [5]. V3 bead data were also scattered, but only on the vertical axis, which was characteristic of different degrees of polymerization, i.e., different temperatures of melting/processing; this could be due to the addition of lead (European origin) or Na/Ca containing fluxes as observed for re-processed glass [5].
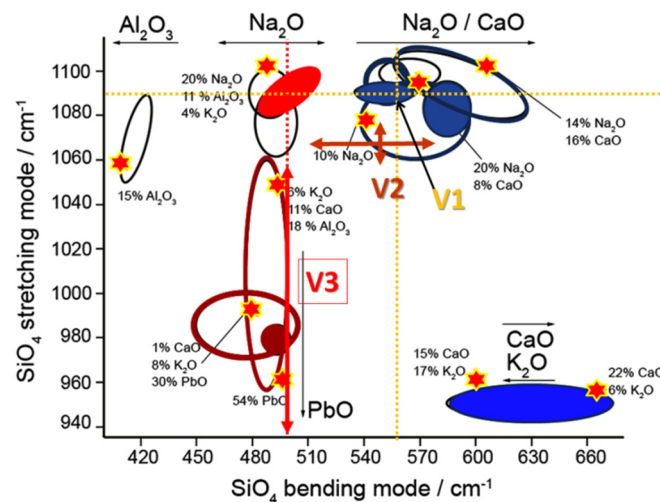
Figure 7. Plot of the maxima of the SiO$_4$ stretching and bending peaks for different glass types. The ellipses delimit the distribution of data for the different families of vitreous silicates used since the origins [50]. The dotted lines and arrows show the wavenumber range of the bending and stretching modes of glass: soda-lime glass (V1/European and V2), lead-substituted glass (V3, cf. Table 2). Raman criteria of classification differ from those of composition (they are firstly related to the degree of polymerization of SiO$_4$ tetrahedron but a link with composition can be made; examples of compositions are given for the points marked with a star (after [50]).

5. Conclusions

This on-site work using a mobile Raman device allowed the identification, as expected, of the crystalline and amorphous phases constituting the beads used to make bracelets and necklaces found in a funeral context. Objective conclusions were made for beads "in good condition," namely, semi-precious stones or non-corroded glass, which were transparent or translucent. The conclusions obtained for the opaque, corroded materials were much more questionable, especially if it was not possible to analyze the bulk through fresh fractures of the objects.

Nevertheless, the dating markers established from the nature of the phases observed in the beads were quite consistent with those made from the decorations of the ceramics found with the beads.

The comparison of the classifications based on a simple visual criterion of all the glass beads from Vohemar kept in Madagascar appeared very different from the set studied in this work. Its representativeness was therefore very limited. We can see how the selection that the amateur archaeologists made in the beginning of the 20th century, no doubt on aesthetic or curiosity criteria, modified the true knowledge.

References

1. Beaujard, P. *Les Mondes de l'océan Indien, Vol. 1, De la Formation de l'État au Premier Système Monde Afro-Eurasien, Vol. 2. L'océan Indien, au Cœur des Globalisations de l'Ancien Monde (7e-15e Siècles)*; Armand Colin: Paris, France, 2012.
2. Francis, P., Jr. *Asia's Maritime Bead Trade, 300BC to the Present*; University of Hawaii Press: Honolulu, HI, USA, 2002.
3. Carswell, J. China and Islam in the Maldives Islands. *Trans. Oriental Ceram. Soc.* **1977**, *41*, 21–198.
4. Rougeulle, A. Golfe Persique et mer Rouge: Notes sur les routes de la céramiques aux Xe-XIIesiècles. *Taoci* **2005**, *4*, 41–51.
5. Koleini, F.; Colomban, P.; Pikirayi, I.; Prinsloo, L.C. Glass Beads, Markers of Ancient Trade in Sub-Saharan Africa: Methodology, State of the Art and Perspectives. *Heritage* **2019**, *2*, 2343–2369. [CrossRef]
6. Koleini, F.; Pikirayi, I.; Colomban, P. Revisiting Baranda: A multi-analytical approach in classifying. sixteenth/seventeenth-century glass beads from northern Zimbabwe. *Antiquity* **2017**, *91*, 751–764. [CrossRef]
7. Fischbach, F.; Ngo, A.T.; Colomban, P.; Pauly, M. Beads excavated from Antsiraka Boira necropolis (Mayotte Island, 12th–13th century); Colouring agents and glass matrix composition comparison with contemporary Southern Africa sites. *Revue d'Archéomètrie Archéosciences* **2016**, *40*, 83–102. [CrossRef]
8. Grandidier, A.; Grandidier, G. *Ethnographie de Madagascar*; tome 1, Impr; Nationale: Paris, France, 1908.
9. Vernier, E.; Millot, J. Archéologie Malgache. In *Comptoirs Musulmans, Catalogues du Musée de l'Homme, Série F, Madagascar, 1*; Supplément à Objets et Monde XI(3); Musée National d'Histoire Naturelle: Paris, France, 1971.
10. Schreurs, G.; Evers, J.T.M.S.; Radimilahy, C.; Rakotoarisoa, J.-A. The Rasikajy civilization in northeast Madagascar: A pre-European Chinese communauty? *Études Océan Indien* **2011**, *46–47*, 107–132. [CrossRef]
11. Vérin, P. *The History of Civilization in North. Madagascar*; Balkema: Rotterdam, The Netherlands; Boston, MA, USA, 1986.
12. Zhao, B. Vers une expertise plus fine et une approche plus historique de la céramique chinoise de la nécropole de Vohémar. *Études océan Indien* **2011**, *46–47*, 92–103. [CrossRef]
13. Amigues, F. La céramique dorée de Valence trouvée à Vohémar. *Études Océan Indien* **2011**, *46-47*, 75–90. [CrossRef]
14. Dewar, R.E.; Wright, H.T. The culture history of Madagascar. *J. World Prehistory* **1993**, *7*, 417–466. [CrossRef]
15. Allibert, C.; Rakotoarsoa, J.-A. Réévaluation du site de Vohémar: Ouverture à d'autres hypothèses. *Études océan Indien* **2011**, *46–47*, 7–12. [CrossRef]

16. Van der Sleen, W.G.N. *Les Collections Malgaches du Musée de Nîmes*; Naturaliste Malgache: Paris, France, 1960.

17. Van der Sleen, W.G.N. *A Handbook on Beads*; Liberty Cap Books: York, PA, USA, 1973.

18. Rasoarifetra, B. Les perles de Vohémar, origine et marqueurs culturels. *Études Océan Indien* **2011**, *46–47*, 178–193. [CrossRef]

19. Robertshaw, P.; Rasoarifetra, B.; Wood, M.; Melchiorre, E.; Popelka-Filcoff, R.S. Glascock Chemical analysis of glass beads in Madagascar. *J. Afr. Archaeol.* **2006**, *4*, 91–109. [CrossRef]

20. Wood, M. Interconnections; Glass Beads and Trade in Southern and Eastern Africa and the Indian Ocean—7th to 16th Centuries AD. Ph.D. Thesis, Uppsala University, Uppsala, Sweden, 2012.

21. Siu, I.; Henderson, J.; Qin, D.; Cui, J.; Ma, H. New light on plant ash glass found in Africa: Evidence for Indian Ocean Silk Road trade using major, minor, trace element and lead isotope analysis of glass from the 15th–16th century AD from Malindi and Mambui, Kenya. *PLoS ONE* **2020**, *15*, e0237612. [CrossRef] [PubMed]

22. McKinnon, E.E.; Brill, R.H. Chemical analyses of some glasses from Sumatra. In *Archaeometry of Glass, Proceedings of the Archaeometry Session of the XIV Intern. Congress on Glass 1986, New Delhi, Sect. 2*; Bhardwaj, H.C., Ed.; India Ceramic Soc: Calcutta, India, 1987; pp. 1–14.

23. Wood, M. Glass beads and Pre-European trade in the Shashe-Limpopo-region. In *Master of Arts Dissertation*; University of the Witwatersrand: Johannesburg, South Africa, 2005.

24. Wood, M. A glass bead sequence for Southern Africa from the 8th to the 16th century AD. *J. Afr. Archaeol.* **2011**, *9*, 67–84. [CrossRef]

25. Wood, M. Glass beads from pre-European contact sub-Saharan Africa: Peter Francis's work revisited and updated. *Archaeol. Res. Asia* **2016**, *6*, 65–80. [CrossRef]

26. Available online: https://en.wikipedia.org/wiki/Chevron_bead (accessed on 22 February 2021).

27. Veiga, J.P.; Figueiredo, M.O. Sixteenth century tubular glass beads: Non-destructive chemical characterization using Synchrotron radiation XRF. *X Ray Spectrum.* **2002**, *31*, 300–304. [CrossRef]

28. Available online: https://www.cmog.org/artwork/nueva-cadiz-bead (accessed on 22 February 2021).

29. Beck, H.C. *Classification and Nomenclature of Beads and Pendants*; Communicated to the Society of Antiquaries: Oxford, UK, 1928.

30. Dubin, L.S. *Histoire des Perles de la Préhistoire à Nos Jours*; Nathan: Paris, France, 1988.

31. Allchin, B. *The Agate and Carnelian Industry of Western India and Pakistan*; Brill, E.J., Ed.; South Asian Archaeology: Leiden, The Neitherland, 1979; pp. 91–105.

32. Kenoyer, J.M.; Vidale, M.; Bhan, K.K. Carnelian production in Khambat India: An ethnoarchaeological study. In *Living Traditions: Studies in the Ethnoarchaeology of South Asia*; Allchin, B., Ed.; Oxford—IBH: New Delhi, India, 1994; pp. 281–306.

33. Roux, V. *Cornaline de l'Inde: Des Pratiques Techniques de Cambay aux Techno-Systèmes de l'Indus*; Editions de la Maison des Sciences de l'homme: Paris, France, 2000.

34. Bellina, B. Beads, social change and interaction between India and South-east Asia. *Antiquity* **2003**, 285–297. [CrossRef]

35. Insoll, T.; Polya, D.A.; Bhan, K.; Irving, D.; Jarvis, K. Towards ans understanding of the carnelian bead trade from Western India to sub-Saharan Africa: The application of UV-LA-ICP-MS to carnelian from Gujarat, India, and West Africa. *J. Archaeol. Sci.* **2004**, *31*, 1161–1173. [CrossRef]

36. Carter, A.K.; Dussubieux, L. Geologic provenience analysis of agate and carnelian beads using laser ablation-inductively coupled plasma-mass spectrometry (LA-ICP-MS): A case study from Iron Age Cambodia and Thailand. *J. Archaeol. Sci. Rep.* **2016**, *6*, 321–331. [CrossRef]

37. Wood, M.; Dussubieux, L.; Robertshaw, P. Glass finds from Chibuene, a 6th to 17th century AD port in southern Mozambique. *S. Afr. Archaeol. Bull.* **2012**, *67*, 59–74.

38. Wood, M.; Panighello, S.; Orsega, E.F.; Robertshaw, P.; van Elteren, J.T.; Crowther, A.; Horton, M.; Boivin, N. Zanzibar and Indian Ocean trade in the first millennium Ce: The glass bead evidence. *Archaeol. Anthropol. Sci.* **2017**, *9*, 879–901. [CrossRef]

39. Bernard-Thierry, S. Inventaire des perles de fouille à Madagascar. *Bull. Académie Malgache* **1957**, *37*, 101–141.

40. Bernard-Thierry, S. Perles magiques à Madagascar. *J. Société Afr.* **1959**, *29*, 33–90. [CrossRef]

41. Schreurs, G.; Rakotoarisoa, J.-A. The archaeological site at Vohemar in a regional geographical and geological context. *Études Océan Indien* **2011**, *46–47*. [CrossRef]

42. Pradines, S. Islamic archaeology in the Comoros: The Swahili and the rock crystal trade with the Abbasid and Fatimid caliphates. *J. Islamic Archaeol.* **2019**, *6*, 109–135. [CrossRef]

43. Tournié, A.; Ricciardi, P.; Colomban, P. Glass corrosion mechanisms: A multiscale analysis. *Solid State Ionics* **2008**, *179*, 2142–2154. [CrossRef]

44. Colomban, P. On-site Raman identification and dating of ancient glasses: A review of procedures and tools. *J. Cult. Herit.* **2008**, *9*, e55–e60. [CrossRef]

45. Colomban, P. Polymerisation degree and Raman identification of ancient glasses used for jewellery, ceramics enamels and mosaics. *J. Non Cryst. Solids* **2003**, *323*, 180–187. [CrossRef]

46. Colomban, P.; Tournié, A.; Bellot-Gurlet, L. Raman identification of glassy silicates used in ceramics, glass and jewellery: A tentative differentiation guide. *J. Raman Spectrosc.* **2006**, *37*, 841–852. [CrossRef]

47. Colomban, P.; Paulsen, O. Non-destructive determination of the structure and composition of glazes by Raman spectroscopy. *J. Am. Ceram. Soc.* **2005**, *88*, 390–395. [CrossRef]

48. Ricciardi, P.; Colomban, P.; Tournié, A.; Milande, V. Non-destructive on-site identification of ancient glasses: Genuine artefacts, embellished pieces or forgeries? *J. Raman Spectrosc.* **2009**, *40*, 604–617. [CrossRef]

49. Caggiani, M.C.; Colomban, P.; Mangone, A.; Valloteau, C.; Cambon, P. Mobile Raman spectroscopy analysis of ancient enamelled glass masterpieces. *Anal. Methods* **2013**, *5*, 4345–4354. [CrossRef]

50. Koleini, F.; Prinsloo, L.C.; Biemond, W.M.; Colomban, P.; Ngo, A.; Boeyens, J.; van der Ryst, M. Towards refining the classification of glass trade beads imported into southern Africa from the 8th to the 16th century AD. *J. Cult. Herit.* **2016**, *19*, 435–444. [CrossRef]

51. Koleini, F.; Colomban, P.; Antonites, A.; Pikirayi, I. Raman and XRF classification of Asian and European glass beads recovered at Mutamba, a southern African Middle Iron Age site. *J. Archaeol. Sci. Rep.* **2017**, *13*, 333–340. [CrossRef]

52. Koleini, F.; Machiridza, L.H.; Pikirayi, I.; Colomban, P. The chronology of Insiza cluster Khami-phase sites in south-western Zimbabwe: Compositional insights from pXRF and Raman analysis of excavated exotic glass finds. *Archaeometry* **2019**, *61*, 874–890. [CrossRef]

53. Prinsloo, L.C.; Colomban, P. A Raman spectroscopic study of the Mapungubwe oblates: Glass trade beads excavated at an Iron Age archaeological site in South Africa. *J. Raman Spectrosc.* **2008**, *39*, 79–90. [CrossRef]

54. Kingma, K.J.; Hemley, R.J. Raman-spectroscopy study of microcrystalline silica. *Am. Mineral.* **1994**, *79*, 269–273.

55. Gotze, J.; Nasdala, L.; Kleeberg, R.; Wenzel, N. Occurrence and distribution of "moganite" in agate/chalcedony: A combined micro-Raman, Rietveld and cathodoluminescence study. *Contr. Mineral. Petrol.* **1998**, *133*, 96–105. [CrossRef]

56. Smith, D.C.; Robin, S. Early Roman Empire intaglios from 'rescue excavations' in Paris: An application of the Raman microprobe to the non-destructive characterization of archaeological objects. *J. Raman Spectrosc.* **1997**, *28*, 189–193. [CrossRef]

57. Roqué-Rosell, J.; Torchy, L.; Roucau, C.; Lea, V.; Colomban, P.; Regert, M.; Binder, D.; Pelegrin, J.; Sciau, P. Influence of Heat Treatment on the Physical Transformations of Flint Used by Neolithic Societies in the Western Mediterranean. *Mater. Res. Soc. Proc.* **2011**, *1319*. [CrossRef]

58. Colomban, P.; Slodczyck, A. The structural and dynamics neutron study of proton conductors: Difficulties and improvement procedures in protonated perovskite. *Eur. Phys. J. Special Topics* **2012**, *213*, 171–193. [CrossRef]

59. Hatipoglu, M.; Tuncer, Y.; Kibar, R.; Cetin, A.; Karali, T.; Can, N. Thermal properties of gem-quality moganite-rich blue chalcedony. *Physica B Cond. Matter* **2010**, *405*, 4627–4633. [CrossRef]

60. Gliozzo, E. Variations on the silica theme: Classification and provenance from Pliny to current supplies. In *Contribution of Mineralogy to Cultural Heritage*; Artioli, G., Oberti, R., Eds.; Book Series: European Mineralogical Union Notes in Mineralogy; The Mineralogical Society: Twickenham, UK, 2019; Volume 20, pp. 13–85. [CrossRef]

61. Joyner, L.; Freestone, I.; Robinson, M. Crowning glory: The identification of gems on the head reliquary of St Eustace from the Basle Cathedral Treasury. *J. Gemmol.* **2006**, *30*, 169–182. [CrossRef]

62. Petrova, Z.; Jehlicka, J.; Capoun, T.; Hanus, R.; Trojek, T.; Golias, V. Gemstones and noble metals adorning the sceptre of the Faculty of Science of Charles University in Prague: Integrated analysis by Raman and XRF handheld instruments. *J. Raman Spectrosc.* **2012**, *43*, 1275–1280. [CrossRef]

63. Kadlecikova, M.; Breza, J.; Vanco, L.; Gregor, M.; Bazovsky, I. Raman Spectroscopy of Ancient Beads from Devin Castle near Bratislava and of Four Intaglios from other Archaeological Finds in Slovakia. *J. Gemmol.* **2015**, *34*, 510–517. [CrossRef]

64. Froment, F.; Tournié, A.; Colomban, P. Raman identification of natural red to yellow pigments: Ochre and iron-containing ores. *J. Raman Spectrosc.* **2008**, *39*, 560–568. [CrossRef]

65. Sakellariou, K.; Miliani, C.; Morresi, A.; Ombelli, M. Spectroscopic investigation of yellow majolica glazes. *J. Raman Spectrosc.* **2004**, *35*, 61–67. [CrossRef]

66. Sandalinas, C.; Ruiz-Moreno, S. Lead-tin-antimony yellow-Historical manufacture, molecular characterization and identification in seventeenth-century Italian paintings. *Stud. Conserv.* **2004**, *49*, 41–52. [CrossRef]

67. Sandalinas, C.; Ruiz-Moreno, S.; Lopez-Gil, A.; Miralles, J. Experimental confirmation by Raman spectroscopy of a Pb-Sn-Sb triple oxide yellow pigment in sixteenth-century Italian pottery. *J. Raman Spectrosc.* **2006**, *37*, 1146–1153. [CrossRef]

68. Rosi, F.; Manuali, V.; Miliani, C.; Brunetti, B.G.; Sgamellotti, A.; Grygar, T.; Hradil, D. Raman scattering features of lead pyroantimonate compounds. Part I: XRD and Raman characterization of $Pb_2Sb_2O_7$ doped with tin and zinc. *J. Raman Spectrosc.* **2009**, *40*, 107–111. [CrossRef]

69. Pereira, M.; de Lacerda-Aroso, T.; Gomes, M.J.M.; Mata, A.; Alves, L.C.; Colomban, P. Ancient Portuguese ceramic wall tiles («Azulejos»): Characterization of the glaze and ceramic pigments. *J. Nano Res.* **2009**, *8*, 79–88. [CrossRef]

70. Kırmızı, B.; Colomban, P.; Blanc, M. On-site analysis of Limoges enamels from sixteenth to nineteenth centuries: An attempt to di_erentiate between genuine artefacts and copies. *J. Raman Spectrosc.* **2010**, *41*, 1240–1247. [CrossRef]

71. Pelosi, C.; Agresti, G.; Santamaria, U.; Mattei, E. Artificial yellow pigments: Production and characterization through spectroscopic methods of analysis. *E Preserv. Sci.* **2010**, *7*, 108–115.

72. Rosi, F.; Manuali, V.; Grygar, T.; Bezdicka, P.; Brunetti, B.G.; Sgamellotti, A.; Burgio, L.; Seccaroni, C.; Miliani, C. Raman scattering features of lead pyroantimonate compounds: Implication for the non-invasive identification of yellow pigments on ancient ceramics. Part II. In situ characterisation of Renaissance plates by portable micro-Raman and XRF studies. *J. Raman Spectrosc.* **2011**, *42*, 407–414. [CrossRef]

73. Cartechini, L.; Rosi, F.; Miliani, C.; D'Acapito, F.; Brunetti, B.G.; Sgamellotti, A. Modified Naples yellow in Renaissance majolica: Study of Pb-Sb-Zn and Pb-Sb-Fe ternary pyroantimonates by X-ray absorption spectroscopy. *J. Anal. At. Spectrom.* **2011**, *26*, 2500–2507. [CrossRef]

74. Kırmızı, B.; Göktürk, H.; Colomban, P. Colouring agents in the pottery glazes of western Anatolia: A new evidence for the use of Naples yellow pigment variations during the late Byzantine period. *Archaeometry* **2015**, *57*, 476–496. [CrossRef]

75. Montanari, R.; Murakami, N.; Colomban, P.; Alberghina, M.F.; Pelosi, C.; Schiavone, S. European Ceramic technology in the Far East: Enamels and pigments in Japanese art from the 16th to the 20th century and their reverse influence on China. *Herit. Sci.* **2020**, *8*, 48. [CrossRef]

76. Colomban, P.; Kırmızı, B.; Gougeon, C.; Gironda, M.; Cardinal, C. Pigments and glassy matrix of the 17th–18th century enamelled French watches: A non-invasive on-site Raman and pXRF study. *J. Cult. Herit.* **2020**, *44*, 1–14. [CrossRef]

77. Hancock, R.G.V.; McKechnie, J.; Aufreiter, S.; Karklins, K.; Kapches, M.; Sempowski, M.; Moreau, J.-F.; Kenyon, I. Non-destructive analysis of European cobalt blue glass trade beads. *J. Radioanal. Nucl. Chem.* **2000**, *244*, 567–573. [CrossRef]

78. Koleini, F.; Prinsloo, L.C.; Biemond, W.; Colomban, P.; Ngo, A.; Boeyens, J.C.; Van der Riest, M.; Van Brakel, K. Unravelling the glass trade bead sequence from Magoro Hill, South Africa: Separating pre-seventeenth-century Asian imports from later European counterparts. *Herit. Sci.* **2016**, *4*, 43. [CrossRef]

79. Colomban, P.; Tournié, A.; Maucuer, M.; Meynard, P. On-site Raman and XRF analysis of Japanese and Chinese bronze/brass patina–the search for specific Raman signatures. *J. Raman Spectrosc.* **2012**, *43*, 799–808. [CrossRef]